This article was downloaded by: *[CAS Consortium]*
On: *9 June 2011*
Access details: *Access Details: [subscription number 937805358]*
Publisher *Taylor & Francis*
Informa Ltd Registered in England and Wales Registered Number: 1072954 Registered office: Mortimer House, 37-41 Mortimer Street, London W1T 3JH, UK

Heat Transfer Engineering
Publication details, including instructions for authors and subscription information:
http://www.informaworld.com/smpp/title~content=t713723051

Seed Bubble Guided Heat Transfer in a Single Microchannel

Jinliang Xu[ab]; Wei Zhang[a]; Guohua Liu[b]
[a] Beijing Key Laboratory of New and Renewable Energy, North China Electric Power University, Beijing, China [b] Micro Energy System Laboratory, Chinese Academy of Sciences, Guangzhou Institute of Energy Conversion, Guangzhou, China

Accepted uncorrected manuscript posted online: 10 February 2011

Online publication date: 09 June 2011

To cite this Article Xu, Jinliang , Zhang, Wei and Liu, Guohua(2011) 'Seed Bubble Guided Heat Transfer in a Single Microchannel', Heat Transfer Engineering, 32: 11, 1031 — 1036, doi: 10.1080/01457632.2011.556493, First posted on: 10 February 2011 (iFirst)
To link to this Article: DOI: 10.1080/01457632.2011.556493
URL: http://dx.doi.org/10.1080/01457632.2011.556493

PLEASE SCROLL DOWN FOR ARTICLE

Full terms and conditions of use: http://www.informaworld.com/terms-and-conditions-of-access.pdf

This article may be used for research, teaching and private study purposes. Any substantial or systematic reproduction, re-distribution, re-selling, loan or sub-licensing, systematic supply or distribution in any form to anyone is expressly forbidden.

The publisher does not give any warranty express or implied or make any representation that the contents will be complete or accurate or up to date. The accuracy of any instructions, formulae and drug doses should be independently verified with primary sources. The publisher shall not be liable for any loss, actions, claims, proceedings, demand or costs or damages whatsoever or howsoever caused arising directly or indirectly in connection with or arising out of the use of this material.

Heat Transfer Engineering, 32(11–12):1031–1036, 2011
Copyright © Taylor and Francis Group, LLC
ISSN: 0145-7632 print / 1521-0537 online
DOI: 10.1080/01457632.2011.556493

Taylor & Francis
Taylor & Francis Group

Seed Bubble Guided Heat Transfer in a Single Microchannel

JINLIANG XU,[1,2] WEI ZHANG,[1] and GUOHUA LIU[2]

[1]Beijing Key Laboratory of New and Renewable Energy, North China Electric Power University, Beijing, China
[2]Micro Energy System Laboratory, Guangzhou Institute of Energy Conversion, Chinese Academy of Sciences, Guangzhou, China

We use the seed bubble concept for manipulating the evaporative heat transfer in a heated microchannel with smooth surfaces. Using this concept, separation of bubble nucleation and growth is obtained to simplify the heat transfer system. Not only is the temperature excursion at the boiling incipience eliminated, but also the heat transfer system displays well-ordered and repeated flow characteristics. The heat transfer rates and wall temperatures can be controlled through adjusting the seed bubble frequency. The method provides a thermal management solution for microsystems and a tool for the study of the intricate flow and heat transfer.

Downloaded By: [CAS Consortium] At: 09:47 9 June 2011

INTRODUCTION

As an efficient heat transfer mode, boiling heat transfer is widely used in information [1], space [2], and biotechnologies [3]. Even though boiling heat transfer has been studied for more than a century, it is still difficult to control due to its random, nonrepeatable, and nonlinear behaviors. However, the rapid development of microfabrication technology in recent years provides a new opportunity to fully control the boiling heat transfer. Here we report a heat transfer mode controlled by a seed bubble generator. The similar idea was proposed by Thome and Dupont [4] in a European patent. In this study we prefer using smooth silicon microchannels; thus, bubble nuclei are never created in the heated microchannels but provided by a seed bubble generator. The experimental results indicate that such a microsystem fully eliminates the temperature excursion at the boiling incipience, and precisely controls the flow patterns and heat transfer in smooth microchannels. Separation of bubble nucleation and growth processes simplifies the heat transfer system and provides a tool for the study of intricate multiphase flow and heat transfer.

This work was supported by the National Science Fund for Distinguished Young Scholars from the National Natural Science Foundation of China (50825603) and the Natural Science Foundation of China (50776089).

Address correspondence to Professor Jinliang Xu, Beijing Key Laboratory of New and Renewable Energy, North China Electric Power University, Beijing 102206, China. E-mail: xjl@ncepu.edu.cn

EXPERIMENTS

Design of the Seed Bubble Guided Heat Transfer System

The microsystem was fabricated by standard MEMS technology. Figure 1a shows the 3D assembly of test section, consisting of a top 7740 glass cover bonded with a silicon substrate, and a heated copper block attached on the back surface of the silicon substrate. Layers of titanium, platinum, and gold films were consecutively sputtered on the back surface of the glass cover. The exposed platinum film (100 μm by 20 μm) was formed after removing the top gold through wet erosion, acting as the seed bubble generator driven by consecutive pulse signals through bonding wires (not shown in the figure). The platinum film exactly faces the chamber center in the silicon substrate. The chamber has the size of 1000 μm by 1000 μm, the inlet and outlet of which are nozzle configurations with diverging angles of 14°, guiding seed bubbles flowing downstream and maintaining them in the microchannel center. The nozzle entrance has a cross section of 40 μm by 40 μm. The whole etched configurations have the same depth of 40 μm. The straight microchannel has a width of 200 μm. In order to characterize flow and heat transfer parameters, a one-dimensional coordinate system was established, shown in Figure 1b. The original point ($z = 0$) starts from the beginning of the heated region, represented by the dashed rectangular box in Figure 1b. The coordinates of other specific points are $z_A = -9.5$ mm, $z_B = -8.0$ mm, $z_o = 0$, $z_C = 11.0$ mm. During operation of

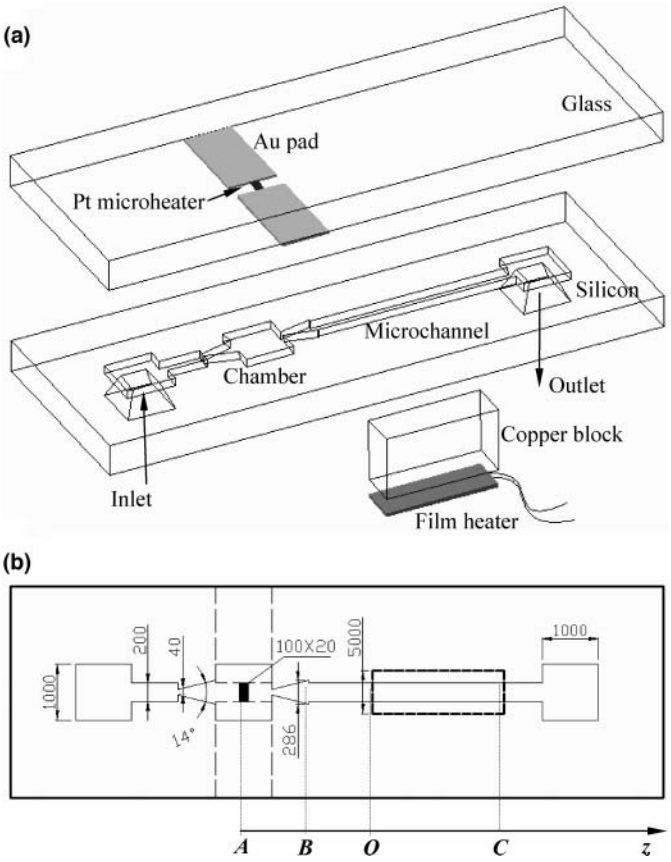

Figure 1 Configurations of seed bubble guided heat transfer microsystem.

the microsystem, the heating area (11.0 mm length by 5.0 mm width) was maintained at a constant temperature T_w, which was adjusted by a PID (proportional/integrated/differential) temperature control unit.

Experimental Setup

As shown in Figure 2, the experimental setup includes a liquid feed system (not shown here), a pulse voltage generator, a temperature control unit, an optical measurement system, and a data acquisition system. The liquid feed system used a syringe pump to supply a constant liquid flow rate into the microsystem. Fine K-type thermocouples were installed at the inlet and outlet of the microsystem to measure fluid temperatures. A pressure drop transducer was arranged across the microsystem. The pulse voltage generator provides pulse heating on the Pt microheater, driving the bubble formation with a frequency from 0.2 Hz to 20 MHz.

The temperature control unit coupled with a DC power supply was used to maintain a constant temperature for the copper block. The optical measurement system consisting of a microscope and a high-speed camera has a temporal resolution of 10 μs and a spatial resolution of 5 μm. The data acquisition system has the maximum recording rate up to 100 MS/s. During the experiments, both the high-speed data acquisition system and the high-speed camera were in the waiting mode. The synchronization hub sends a signal, triggering functions of both systems. The maximum time delay between the two synchronized systems is smaller than 20 ns. For all experiments, the microsystem was horizontally positioned. Pure degassed methanol liquid was used as the working fluid.

DATA REDUCTION

The microheater temperature calibration process was similar to that reported in our recent paper [5]. Here the correlation between the resistance (R_{film}) and temperature (T_{film}) of the Pt film microheater was deduced as $R_{film} = 0.00168\ T_{film} + 7.39$, which is valid over the range from 5 to 120°C.

For a specific cross section, the transient axial void fraction $\alpha(z,t)$ was computed as the vapor width relative to the channel width. Corresponding to the seed bubble generation cycle period, the time-averaged void fraction was computed as

$$\langle\alpha\rangle_z = \int_t^{t+\tau} \alpha(z,t)dt/\tau \tag{1}$$

The heat transfer rate was computed from the inlet to the location of $z = 7.5$ mm (see the coordinate shown in Figure 1b). Fluid at the inlet is single-phase liquid, while fluid at $z = 7.5$ mm is a two-phase mixture. Heat transfer rate should be

$$Q_h = m[xh_v + (1-x)h_f - h_{f,room}] \tag{2}$$

where m is the mass flow rate, x is the vapor mass quality at $z = 7.5$ mm, $x = 1/[1 + (1/\langle\alpha\rangle - 1)\rho_f/\rho_v]$, $\langle\alpha\rangle$ is computed at $z = 7.5$ mm, ρ_f and ρ_v are the densities of liquid and vapor, h_v is the saturated vapor enthalpy, h_f is the superheated liquid enthalpy at $z = 7.5$ mm, and $h_{f,room}$ is the liquid enthalpy at the room temperature of 28°C.

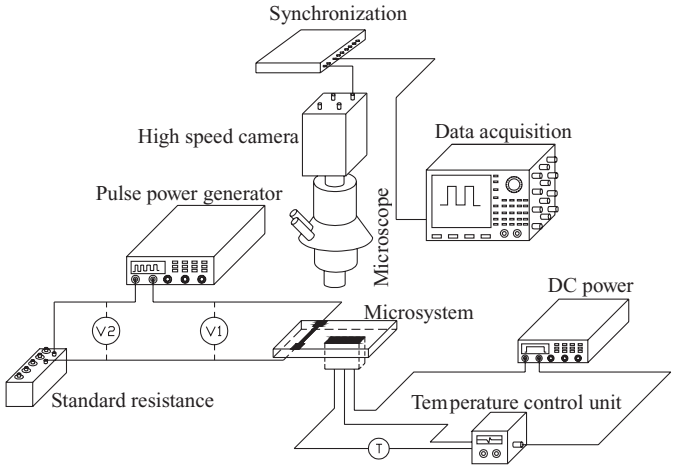

Figure 2 Experimental setup.

Downloaded By: [CAS Consortium] At: 09:47 9 June 2011

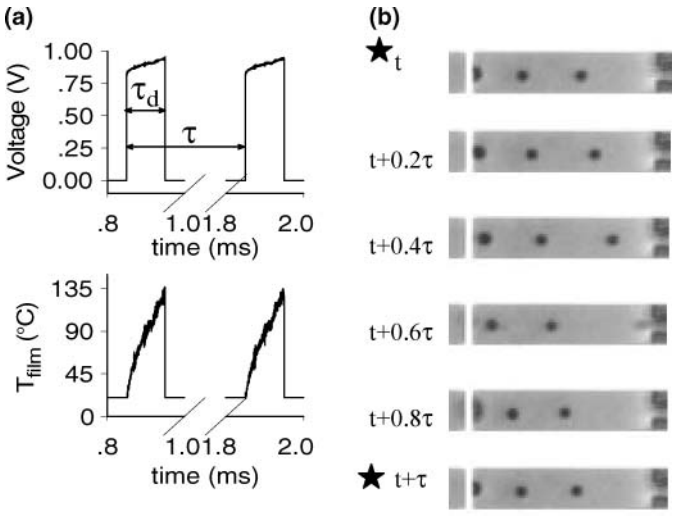

Figure 3 (a) Voltage and temperature response of the thin platinum film heater. (b) Repeated seed bubble generation on the thin film heater. For (a) and (b), Q = 14.0 ml/h, f = 1000 Hz (τ = 1.0 ms).

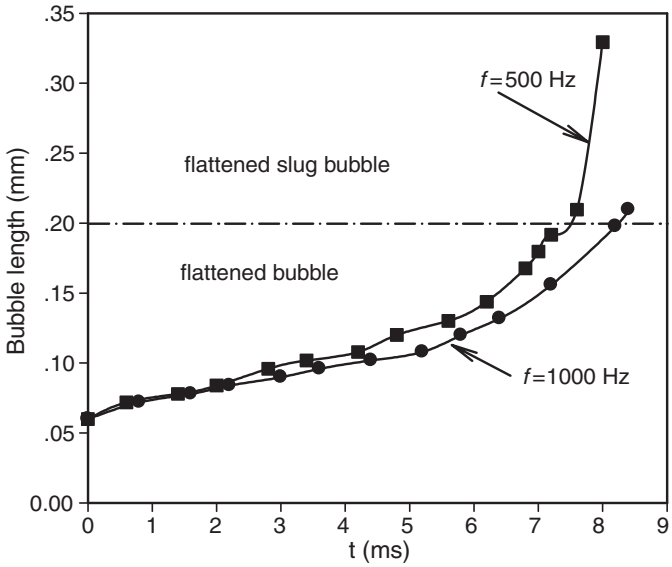

Figure 4 Bubble length versus time at different seed bubble generation frequencies (Q = 14 ml/h,T_w = 66.4°C).

RESULTS AND DISCUSSION

Suppression of Bubble Nucleation in Heated Microchannel

For homogeneous nucleation in ideally smooth or fully wettable channels, bubble nucleation would not take place until the liquid acquires the superheat limit temperature ($0.9T_c$, according to reference [6]). For heterogeneous nucleation, smaller surface roughness always leads to higher boiling incipience temperature. Thus, it is sure that a decrease in surface roughness is always helpful for suppression of bubble nucleation. A microchannel fabricated by standard MEMS technologies usually has a surface roughness ranging from 2 nm to 200 nm, depending on the specific fabrication procedures. Well-controlled fabrication technique easily maintains the surface roughness on the order of several nanometers, which is comparable to the critical bubble nucleation size, suppressing bubble nucleation.

On the other hand, assuming the validity of the no-slip boundary condition, decreases in channel size induce large shear stress on the channel surface due to the large velocity gradient, further suppressing bubble nucleation [7]. In summary, suppression of bubble nucleation at the channel wall can be acquired by using perfectly smooth microchannels, high flow rates, and pure degassed liquids.

Bubble Dynamics on the Seed Bubble Generator

The boiling heat transfer behavior in heated microchannels depends on the precise control of seed bubbles produced on the Pt microheater, provided the bubble nucleation is fully prohibited on the wall surface. This can be achieved by using perfectly smooth microchannels, high flow rates, and pure degassed liquids. Bubble dynamics on a microheater immersed in a stationary pool liquid were experimentally investigated by Xu and Zhang [5]. Bubble formation can be controlled through regulating the voltage applied on the microheater, producing Joule heating for bubble nucleation. When the voltage applied on the microheater is equal to or slightly larger than the critical value triggering bubble nucleation, a single bubble for each pulse cycle can be obtained, under which the bubble formation frequency is exactly equal to the pulse voltage frequency. Much high pulse voltage yields several bubble generation processes during one pulse cycle. Bubble dynamics on microheaters under the flow condition need higher pulse voltage than under the pool boiling condition.

Figure 3 shows the periodic bubble formation and detachment process under the pulse heating condition. Single bubble formation during one pulse is ensured by careful selection of the pulse voltage. The instantaneous heat flux on the microheater was sufficiently high in the range of 10–100 MW/m^2. The formed bubble on the microheater did not detach until the pulse voltage was turned off. The Marangoni force always keeps the bubble on the microheater due to the high temperature of the microheater during the pulse on [8], but it disappears due to the receded temperature during the pulse off. A shear force from the flowing stream detaches the bubble away from the microheater. This process is repeated for different pulse cycles.

Seed Bubble Guided Heat Transfer in Heated Microchannel

Three parameters governing the seed bubble guided heat transfer are the seed bubble frequency f (identical to the pulse frequency), silicon wall temperature T_w, and flow rate Q. The rectangular area in Figure 1b was maintained at a constant temperature T_w. Other surfaces exposed in the air environment were assumed to have a natural convective heat transfer coefficient of 10 W/m-K. In order to verify that the evaporative heat transfer can be triggered at a sufficient low superheat, T_w was selected

Downloaded By: [CAS Consortium] At: 09:47 9 June 2011

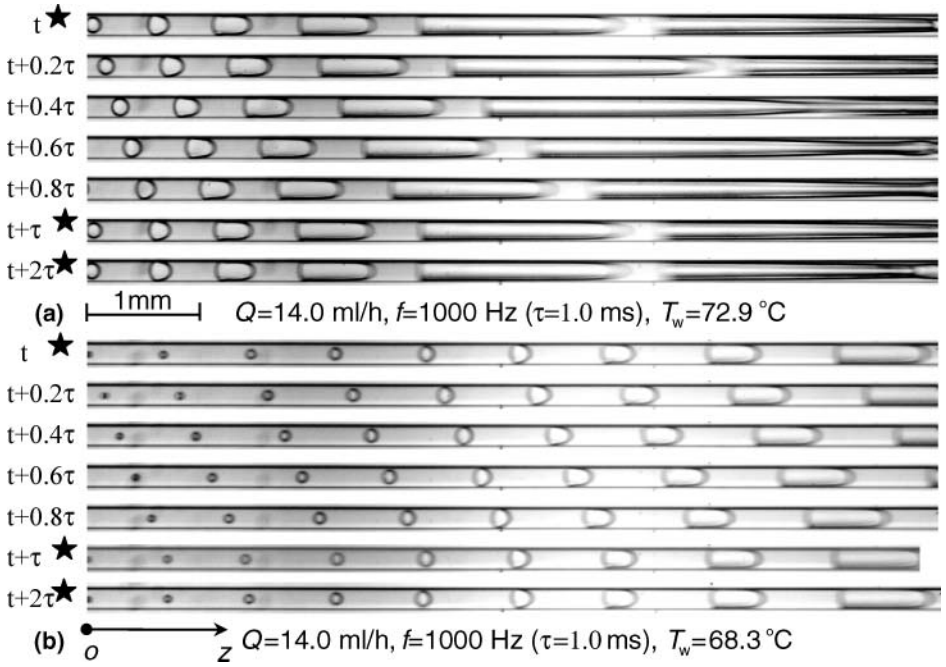

Figure 5 Well-ordered and repeated flow patterns in the microchannel from $z = 0$ to $z = 7.5$ mm. In (a) and (b), images are exactly repeated at t, t + τ, and t + 2τ.

Downloaded By: [CAS Consortium] At: 09:47 9 June 2011

as 66.4°C, slightly larger than the saturation temperature of methanol at atmospheric pressure ($T_{sat} = 64.7$°C at 101.3 kPa). Simulation results show that the liquid was heated from room temperature to about 65°C at $z = 0$ due to the axial thermal conduction. Local liquid superheat varied from 0.3°C at $z = 0$ to 1.6°C at $z = 7.5$ mm. Tracking the growth of a single bubble versus time, the growth rate at $f = 500$ Hz is larger than that at $f = 1000$ Hz (Figure 4), implying a decreased degree of thermal nonequilibrium between liquid and vapor phases with increasing the seed bubble frequency. It is noted that the microchannel has a planar structure with width of $W = 200$ mm and depth of $\delta = 40$ mm. Bubbles in the microchannel have three types of shapes: a spherical bubble for $l < \delta$, which can only be observed at $z < 0$ shown in Figure 3b, a flattened bubble for $\delta < l < W$, and a flattened slug bubble for $l > W$. Here l is the bubble length in the z direction. The flattened slug bubble can only be enlarged in the flow direction due to the confinement of the bubbles in the width and depth directions.

Covering the flow rate range here, we did not find any bubbles in the heated microchannel for the wall superheat up to 15°C. The seed bubble controlled flow patterns in the microchannel depend on f, T_w, and Q. Effects of the wall temperatures on flow patterns are shown in Figures 5a and b, where the higher wall temperature leads to larger bubble growth rate and earlier

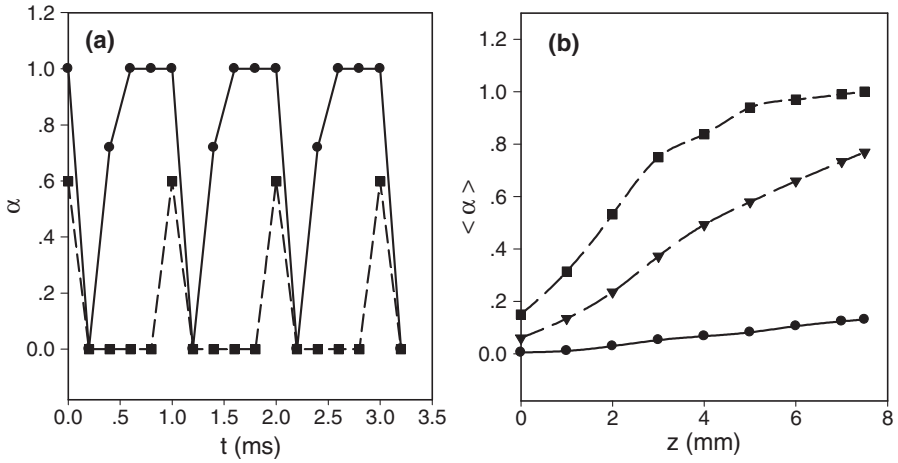

Figure 6 (a) Void fraction versus time at $z = 3.0$ mm: • for $Q = 14.0$ ml/h, $f = 1000$ Hz, $T_w = 72.9$°C, (■) for $Q = 14.0$ ml/h, $f = 1000$ Hz, $T_w = 68.3$°C. (b)Time-averaged void fraction along the z direction. Flow rate Q is 14.0 ml/h: (■) are for $T_w = 72.9$°C, $f = 1000$ Hz, (▼) for $T_w = 72.9$°C, $f = 100$ Hz, • for $T_w = 72.9$°C, $f = 10$ Hz, (▲) for $T_w = 68.3$°C, $f = 1000$ Hz.

Downloaded By: [CAS Consortium] At: 09:47 9 June 2011

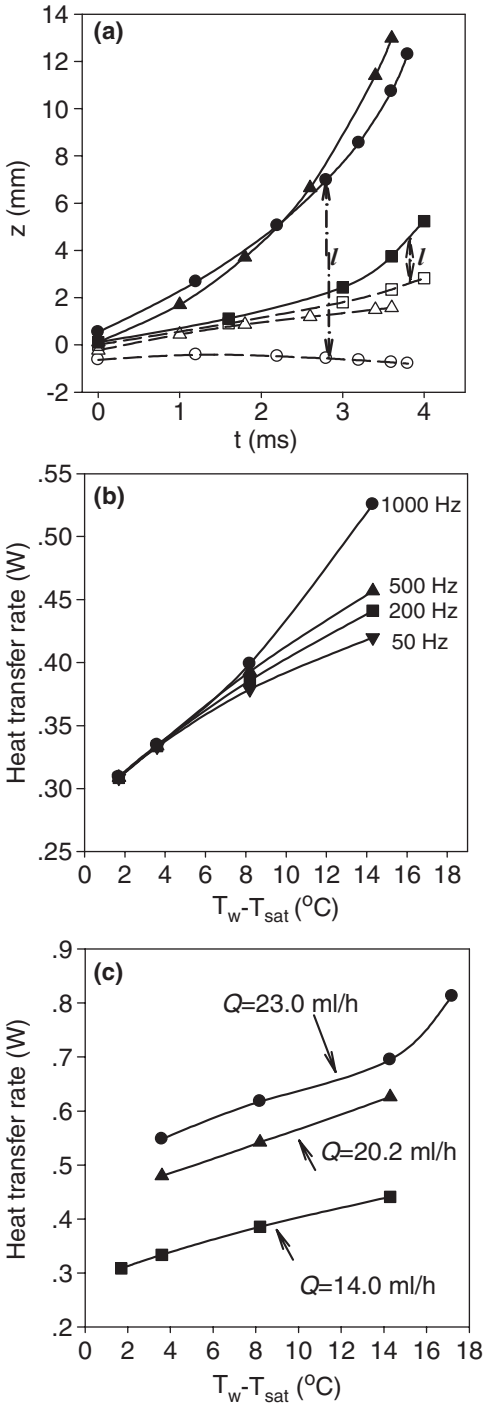

Figure 7 (a) Seed bubble frequency dependent bubble front and rear interface locations. Solid symbols are for front interfaces, open symbols for rear interfaces, circular symbols for $f = 10$ Hz, triangle symbols for $f = 100$ Hz, square symbols for $f = 1000$ Hz. (b) Seed bubble frequency dependent boiling curves. Q is 14.0 ml/h. T_{sat} is the saturation temperature at 101.3 kPa. (c) Flow-rate-dependent boiling curves when seed bubble frequency $f = 200$ Hz.

transition from slug flow to annular flow. Flow patterns at time t are exactly reconstructed at $t + n\tau$, where n is the pulse cycle number; $\tau = 1/f$. Elongated bubble flow ensures thin film evaporation heat transfer in the microchannel, enhancing the heat transfer.

To quantify the repeated flow parameters, we define a cross-sectional void fraction $\alpha(z,t)$, assuming three types of values: $\alpha(z,t) = 1$ if the cross section at z is fully occupied by vapor, $0 < \alpha < 1$ if it is partially occupied by vapor, and $\alpha = 0$ once it is fully occupied by liquid. At the liquid flow rate of $Q = 14$ ml/h and the location of $z = 3$ mm, we study the influence of wall temperatures on the void fractions. Figure 6a shows the void fractions for three consecutive pulse cycles at wall temperatures of 68.3°C and 72.9°C. Here the void fraction is calculated as the bubble width relative to the channel width. Higher wall temperatures always yield larger void fractions. Void fractions at different wall temperatures are well repeated for different cycles, i.e., $\alpha(z,t) = \alpha\ (z,t + n\tau)$. This is impossible in any conventional boiling systems. Then we study the effect of seed bubble frequencies on the time averaged void fractions in Figure 6b at a flow rate of14.0 ml/h and a wall temperature of 72.9°C. The time averaged void fractions calculated by Eq. (1) are increased along the flow direction. Higher seed bubble frequencies always lead to larger void fractions.

We studied the heat transfer rates controlled by seed bubbles and flow rates. Figure 7a shows displacements of front and rear bubble interfaces versus time for $Q = 20.2$ ml/h and $T_w = 79.0$°C, at three seed bubble frequencies of 10, 100, and 1000 Hz. Tracking a bubble from $z = 0$ shows the fastest bubble expansion at $f = 10$ Hz, and slowest expansion at $f = 1000$ Hz. This implies the thermal nonequilibrium between two phases is strongly dependent on seed bubble frequencies. A large degree of thermal nonequilibrium between liquid and vapor phases yields fast bubble growth. Figure 7b shows boiling curves dependent on seed bubble frequencies. Using high seed bubble generation frequencies, large heat transfer rates can be achieved at a given wall temperature and flow rate This phenomenon is similar to that in which boiling heat transfer can be enhanced by increasing the bubble nucleation sites in conventional boiling systems. However, bubble nucleation sites are randomly distributed and cannot be changed artificially. Alternatively, when the heat transfer rate (or the heat flux) is fixed, an expected wall temperature can be obtained by selecting a suitable seed bubble frequency without change to the flow rate (Figure 7b). We call this the seed bubble guided heat transfer mode. Figure 7c shows the increased heat transfer rates with increases in flow rates at the seed bubble frequency of 200 Hz, indicating the commonly used convective heat transfer mode still existing in the present heat transfer system.

CONCLUSIONS

We use the seed bubble concept for heat transfer control. Self-bubble nucleation in the heated channel can be fully prevented by using a smooth silicon channel surface, pure liquids, and high flow rates, provided that wall superheats are not sufficiently large. Seed bubbles can successfully trigger the evaporation heat transfer in the heated channel, even at very low wall superheats, providing a strategy to fully eliminate temperature excursions

in boiling systems. Flow patterns are well ordered and repeated. Seed bubble frequencies control the heat transfer rates at a given wall temperature. Seed bubble frequencies also control wall temperatures without change to the flow rate when heat flux is fixed. The thermal nonequilibrium between vapor and liquid phases is well controlled by seed bubble frequencies. A chaotic boiling system is simplified to a simple one, providing a tool to study the intricate heat transfer, and a thermal management solution for microsystems. It is noted that this is a preliminary study of seed bubble guided heat transfer. More data will be achieved in the future.

NOMENCLATURE

f seed bubble frequency (Hz)
h enthalpy (J/kg)
l bubble length (mm)
Q flow rate (ml/h)
Q_h heat transfer rate (W)
R resistance (Ω)
t time (ms)
T temperature (°C)
z the coordinates of flow direction (mm)

Greeks Symbols

α void fraction
δ channel depth (mm)
ρ density of liquid (kg/m^3)
τ pulse period (ms)

Subscripts

c critical
d duration
f fluid
film film microheater
f room fluid at room temperature
V vapor
W wall
sat saturation

REFERENCES

[1] Thome, J. R., Boiling in Microchannels, A Review of Experiment and Theory, *International Journal of Heat and Fluid Flow*, vol. 25, pp. 128–139, 2004.
[2] Maurya, D. K., Das, S., and Lahiri, S. K., Silicon MEMS Vaporizing Liquid Microthruster With Internal Microheater, *Journal of Micromechanics and Microengineering*, vol. 15, pp. 966–970, 2005.
[3] Daniel, S., Chaudhury, M. K., and Chen, J. C., Fast Drop Movements Resulting From the Phase Change on a Gradient Surface, *Science*, vol. 291, pp. 633–636, 2001.
[4] Thome, J. R., and Dupont, V., Heat Transfer Assembly, European Patent, no. EP 1 779 052 B1, 02.05, 2007.
[5] Xu, J. L., and Zhang, W., Effect of Pulse Heating Parameters on the Microscale Bubble Dynamics at a Microheater Surface, *International Journal of Heat and Mass Transfer*, vol. 51, pp. 389–396, 2008.
[6] Delhaye, J. M., and McLaughlin, J. B., Report of Study Group on Microphysics, *International Journal of Multiphase Flow*, vol. 29, pp. 1101–1116, 2003.
[7] Li, J., and Cheng, P., Bubble Cavitation in a Microchannel, *International Journal of Heat and Mass Transfer*, vol. 47, pp. 2689–2698, 2004.
[8] Takahashi, K., Weng, J. G., and Tien, C. L., Marangoni Effect in Microbubble Systems, *Microscale Thermophysical Engineering*, vol. 3, pp. 169–182, 1999.

Jinliang Xu is a professor at North China Electric Power University. He received his Ph.D. degree in thermal engineering at the State Key Laboratory of Multiphase Flow, Xian Jiaotong University, in 1995. He founded Micro Energy System Laboratory at Guangzhou Institute of Energy Conversion, Chinese Academy of Sciences, in 2002. He has more than 40 refereed papers published in international journals. In April 2009, he joined North China Electric Power University and has been the director of the Beijing Key Laboratory of New and Renewable Energy. His research interests include new and renewable energy, thermal Microsystems, and optical measurements for microsystems.

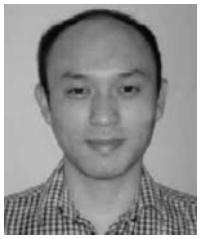

Wei Zhang is an associate professor at North China Electric Power University, China. He received his Ph.D. degree from Guangzhou Institute of Energy Conversion, Chinese Academy of Sciences, in 2008. He worked as a postdoctoral associate on a multiphase microreactor at Eindhoven University of Technology, the Netherlands, from 2008 to 2009. He joined the Beijing Key Laboratory of New and Renewable Energy at North China Electric Power University in May 2009. His current research interests involve renewable energy and microscale heat transfer.

Guohua Liu is a Ph.D. student at Guangzhou Institute of Energy Conversion, Chinese Academy of Sciences. He received his M.S. degree in HVAC (heating, ventilation, and air conditioning) from Xian University of Architecture and Technology. His current research interest is microscale flow and heat transfer.

Downloaded By: [CAS Consortium] At: 09:47 9 June 2011